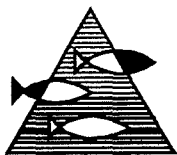


# PROSJEKTRAPPORT

ISSN 0071-5638



## HAVFORSKNINGSINSTITUTTET

MILJØ - RESSURS - HAVBRUK

Nordnesparken 2 Postboks 1870 5024 Bergen

Tlf.: 55 23 85 00 Faks: 55 23 85 31

Forskningsstasjonen

Flødevigen

4817 His

Tlf.: 37 05 90 00

Faks: 37 05 90 01

Austevoll

Havbruksstasjon

5392 Storebø

Tlf.: 56 18 03 42

Faks: 56 18 03 98

Matre

Havbruksstasjon

5198 Matredal

Tlf.: 56 36 60 40

Faks: 56 36 61 43

Distribusjon:

ÅPEN

HI-prosjektnr.:

0302

Oppdragsgiver(e):

NFR

Oppdragsgivers referanse:

Rapport:

FISKEN OG HAVET

NR. 9 - 1997

Tittel:

Simulation of drift of capelin larvae in the Barents Sea

Senter:

Marint miljø

Seksjon:

Fysisk oseanografi

Forfatter(e):

Gro Eriksrød and Bjørn Ådlandsvik

Antall sider, vedlegg inkl.:

33

Dato:

23.09.1997

Sammendrag:

A model system consisting of a regional ocean circulation model and a particle-based larval transport model has been used to study the drift of capelin larvae in the Barents Sea. The modelled current pattern reproduces the important features in the Norwegian Coastal Current and the Norwegian Atlantic Current.

For the four seasons 1988-91 particles were released at 11 spawning areas along the Troms-Finnmark-Kola coast. The particle trajectories from the model do not reproduce the offshore extent of the observed distributions of 0-group capelin in August/September. No clear reason for this discrepancy between the model results and the observations is found, but several factors are discussed.

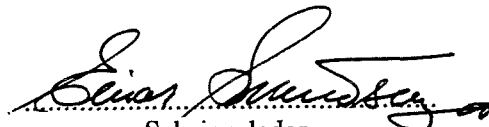
Emneord - norsk:

1. Lodde
2. Larvedrift
3. Barentshavet

Emneord - engelsk:

1. Capelin
2. Larval drift
3. Barents Sea

  
Prosjektleder

  
Seksjonsleder

12 5048



# Simulation of drift of capelin larvae in the Barents Sea

Gro Eriksrød and Bjørn Ådlandsvik

Institute of Marine Research

P.O.Box 1870, Nordnes

N-5024 Bergen, Norway

## **Abstract**

A model system consisting of a regional ocean circulation model and a particle-based larval transport model has been used to study the drift of capelin larvae in the Barents Sea. The modelled current pattern reproduces the important features in the Norwegian Coastal Current and the Norwegian Atlantic Current.

For the four seasons 1988–91 particles were released at 11 spawning areas along the Troms-Finnmark-Kola coast. The particle trajectories from the model do not reproduce the offshore extent of the observed distributions of 0-group capelin in August/September. No clear reason for this discrepancy between the model results and the observations is found, but several factors are discussed.



# CONTENTS

<b>SUMMARY</b>	<b>1</b>
<b>SAMMENDRAG</b>	<b>3</b>
<b>1 INTRODUCTION</b>	<b>5</b>
<b>2 THE CIRCULATION MODEL</b>	<b>7</b>
2.1 Generalities . . . . .	7
2.2 Model setup . . . . .	7
<b>3 THE LARVAE TRANSPORT MODEL</b>	<b>10</b>
3.1 Generalities . . . . .	10
3.2 Model setup . . . . .	10
<b>4 RESULTS FROM THE CIRCULATION MODEL</b>	<b>13</b>
4.1 Current conditions . . . . .	13
4.2 Horizontal diffusion coefficient . . . . .	13
<b>5 RESULTS FROM THE TRANSPORT MODEL</b>	<b>17</b>
5.1 Comparison with observations . . . . .	17
5.2 Comparison of different horizontal diffusion parametrisations . . . . .	23
5.3 Comparison of different vertical migration schemes . . . . .	26
<b>6 DISCUSSION AND CONCLUSION</b>	<b>28</b>
<b>BIBLIOGRAPHY</b>	<b>30</b>



## SUMMARY

A model system consisting of a circulation and a larval transport model has over the last years been used at the Institute of Marine Research (IMR) for simulations of larval drift. In this study the system is applied to the drift of capelin larvae along the coast of Northern Norway and in the Barents Sea. The circulation model, which is based on the Princeton Ocean Model, is set up on a grid area covering the North Sea, the Norwegian Sea and the Barents Sea. The horizontal resolution of the model is 20 km. The vertical has been divided into 14 levels where the distance between the levels depends on the depth. Input data has been taken from a climatological data set produced by the IMR and the Norwegian Meteorological Institute (DNMI). The meteorological forcing has been delivered from DNMI's Hindcast archive.

The model has been run from 15 November the year before to 31 December for the years 1988–91. A comparison with a general circulation pattern based on observations gives a qualitatively good agreement between the model results and the observations. The model shows the Coastal Current along the coast of Northern Norway and the splitting of the Norwegian Atlantic Current into the West-Spitzbergen Current and the North Cape Current. The main difference is the relatively weak inflow of Arctic Water between Spitzbergen, Franz Josef land and Novaya Zemlya in the model results.

Daily (25 hour) mean current velocity fields have been extracted from the circulation model to run the transport model. The knowledge of spawning grounds and periods each year is limited and for this reason the larvae are released in the same areas and with the same hatching curves in all simulations. The larvae are released in 11 spots along the coast where spawning previously has taken place. The releases start on 24 April and last for 15 days with maximum release in the middle of the period.

The results from the model simulations have been compared with 0-group capelin distributions in August/September charted by IMR. This comparison involves the distribution of larvae and the drift pattern and not the actual amount of larvae. In general the agreement between the model results and the observations is not very good. The observations show that in August/September the larvae may be distributed over large parts of the Barents Sea and in the area along the shelf edge up to the west coast of Spitzbergen. In some years the model transports larvae mainly released at Andenes northwards along the shelf edge but these have not been transported as far north as the observations show. Another important issue is the observed

distributions of larvae in large parts of the Barents Sea which has not been reproduced by the model. This means that the model only to a very limited degree is able to transport the larvae north-northeastwards out from the coast of Troms and Finnmark into the Barents Sea.

Simulations with varying horizontal diffusion and varying vertical migration scheme of the larvae have not significantly altered this result. The lacking transport can result from different conditions: The transport model has been run with 25 hour mean current velocities which explicitly filter out the tidal current, or the grid resolution is too crude to represent small scale phenomena. The larvae are to a limited degree able to move horizontally but this cannot alone explain the drift north-northeastwards seen in the observations.

## SAMMENDRAG

Et todelt modellsystem bestående av en sirkulasjons- og en larvetransportmodell er i de senere år benyttet ved Havforskningsinstituttet (HI) til simulering av larvedrift. I dette tilfellet er systemet brukt til drift av loddelarver langs kysten av Nord Norge og i Barentshavet. Sirkulasjonsmodellen, basert på Princeton Ocean Model, er satt opp på et gridområde som dekker Nordsjøen, Norskehavet og Barentshavet. Modellen har en horisontal oppløsning på 20 km mens den vertikalt er delt inn i 14 nivåer hvor avstanden mellom nivåene avhenger av dybden. Inngangsdata er tatt fra et klimatologisk datasett produsert av HI og Det Norske Meteorologiske Institutt (DNMI). De meteorologiske drivkreftene er hentet fra DNMI's Hindcast arkiv.

Modellen er kjørt fra 15. november året før til 31. desember for årene 1988–91. En sammenligning med et generelt strømbilde for Barentshavet basert på observasjoner viser en kvalitativ god overensstemmelse mellom modellresultater og observasjoner. Modellen viser tydelig Kyststrømmen langs kysten av Nord Norge og delingen av den norske Atlanterhavsstrømmen i Vest Spitsbergen strømmen og Nordkappstrømmen. Hovedforskjellen ligger i den relativt svake innstrømning av arktisk vann mellom Spitsbergen, Franz Josef land og Novaja Zemlja i modellresultatene.

Fra sirkulasjonsmodellen er det hentet ut daglige (25 timer) midlere strømhastighetsfelter i Barentshavet og nordøstlige del av Norskehavet til å drive larvetransportmodellen. På grunn av begrensede kunnskaper om gytefelter og gytetidspunkt hvert enkelt år brukes samme utslippsområder og klekkekurver alle fire årene. Larvene slippes i 11 punkter langs kysten hvor gyting tidligere har funnet sted. Utslippene starter 24. april og foregår i en 15 dagers periode med maksimale utslipp midt i perioden.

Resultatene fra modellkjøringene er sammenlignet 0-gruppefordelingene av lodde i august/september kartlagt av Havforskningsinstituttet. Denne sammenligningen går på fordelingsmønster og drift og ikke på mengden larver. Det viser seg at det generelt sett ikke er noen god overensstemmelse mellom modellresultater og observasjoner. Observasjonene viser at i august/september kan larvene være fordelt over store deler av Barentshavet og i området langs eggakanten opp til vest for Spitsbergen. I enkelte år gir modellen transport av larver hovedsakelig sluppet ved Andenes, nordover langs eggakanten, men larvene er ikke fraktet like langt nord som observert. Et annet viktig punkt er at modellens larvefordelinger ikke på langt nær dekker så stor del av Barentshavet som observert. Dette betyr at modellen i liten grad er i stand til reproducere

driften av loddelarver nord-nordøstover ut fra Troms- og Finnmarkskysten. Forsøk med variasjon av horisontal diffusjon og larvenes vertikale bevegelse gir ingen vesentlig endringer. Den manglende transporten kan skyldes flere forhold: Transportmodellen bygger på 25 timers midlede strømhastigheter slik at tidevannsstrømmer ikke er representert eller at gridoppløsningen er for grov til å fange opp småskala fenomener. Larvene er i begrenset grad i stand til å bevege seg horisontalt, men dette alene er ikke nok til å forklare den observerte driften nord-nordøstover.

# 1. INTRODUCTION

Capelin (*Mallotus villosus*) is an important pelagic fish stock in the Barents Sea. General overviews of the Barents Sea capelin can be found in the Pro Mare book (Sakshaug *et al.*, 1994) (in Norwegian) and (Gjøsæter, 1995) (in English). A summary of some of the knowledge on capelin larvae is given in Fossum & Øiestad (1991). In early spring the mature capelin migrates from the Barents Sea to spawn along the coast. The locations of spawning vary greatly from year to year. Some years the spawning can take place as far west as Lofoten, while other years it can occur along the easternmost coast of Finnmark and the coast of the Kola peninsula. After hatching the larvae drift with the current and become spread out in the open Barents Sea.

Modelling of adult capelin is done both at the Institute of Marine Research (IMR) and the department of Fisheries and Marine Biology at the University of Bergen (IFM). At IMR capelin is an integrated part of the multi-species modelling project (Tjelmeland & Bogstad, 1993; Bogstad *et al.*, 1997). At IFM a fitness-based approach is used (Giske *et al.*, 1992; Fiksen *et al.*, 1995). The background for the present work is to complement the two above-mentioned modelling projects with a model of the larval stage of capelin. The objective is to simulate the drift of the capelin larvae from the coast, and thereby provide information on where good spawning areas are located and where the spawning took place in different years.

The numerical model system at the Institute of Marine Research (IMR) has previously been used in studies of sandeel larvae in the North Sea (Berntsen *et al.*, 1994), cod larvae in the Barents Sea (Ådlandsvik & Sundby, 1994), herring larvae along the Norwegian coast (Svendsen *et al.*, 1995), polar cod larvae in the Barents Sea (Hansen & Ådlandsvik, 1996), blue whiting larvae hatched along the west coast of Ireland and northwest of Scotland (Svendsen *et al.*, 1996) and herring larvae in the North Sea (Moksness *et al.*, 1997). The work reported here is an application of the same methods to capelin larvae in the Barents Sea. It is part of a larger cooperative project on capelin modelling between IFM and IMR. This report presents the results from the numerical simulations and comparisons of these with observed distributions.

In the transport model the capelin larvae are released as particles at sites where spawning has been known to take place. The transportation of the particles in the model are done with current fields delivered by a circulation model which has been run in an area covering the Norwegian Sea, the Barents Sea and the North Sea.

## **Acknowledgement**

The authors would like to thank Harald Gjøsæter for his valuable help. This work has been partly financed by the Norwegian Research Council by a subcontract from IFM.

## 2. THE CIRCULATION MODEL

### 2.1 Generalities

The numerical model used in this study is the well-known Princeton Ocean Model (POM) developed by Blumberg & Mellor (1987) with modifications done at The Norwegian Meteorological Institute (DNMI) and the Institute of Marine Research (IMR). This is a 3D baroclinic ocean model, with the surface elevation, velocity, salinity, temperature and two variables for vertical mixing as model variables. In addition to the initial and boundary description of the model variables, the model forcing may include wind stress, air pressure, heat exchange with the atmosphere, tidal forcing, and river run-off.

The model solves the primitive equations numerically by the finite differences method. In the vertical terrain following  $\sigma$ -coordinates are used. The model uses mode splitting between the external gravity wave mode and the internal baroclinic mode. The Leapfrog technique is used to step forward in time. For vertical mixing, a Mellor-Yamada level 2.5 turbulence closure scheme is used (Mellor & Yamada, 1982).

The most important modification from the standard POM version is the use of the Flow Relaxation Scheme (FRS) as open boundary condition. This method is documented in Martinsen & Engedahl (1987) and the implementation in POM is documented in Engedahl (1995). Most of the other modifications are related to data handling, and should not influence the numerical solution. The model system at IMR including integrated chemical and biological components is covered in larger detail by Skogen (1993).

### 2.2 Model setup

The setup of the circulation model is documented in more detail by Ådlandsvik & Eriksrød (1997). The model domain is shown in fig. 2.1. The horizontal resolution is 20 km and the number of grid cells is  $208 \times 120$ . The model has been run from 15 November the year before until 31 December for the four years 1988-91.

In the vertical 14  $\sigma$ -levels are used, with  $\sigma$ -coordinates 0., -0.005, -0.012, -0.025, -0.05, -0.1, -0.15, -0.2, -0.3, -0.4, -0.6, -0.8, -0.95, -1. The external time-step is 30 seconds and the internal

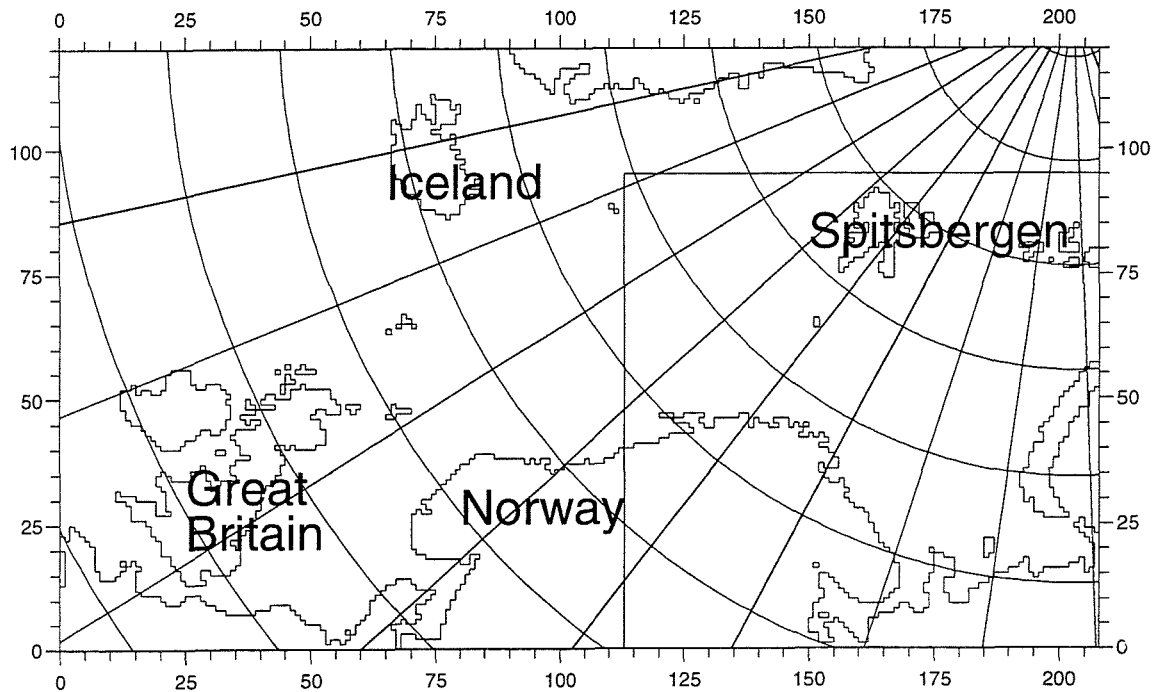


Figure 2.1: The circulation model domain with the domain used in the transport model marked in the right part (see fig. 3.1).

time-step is 15 minutes.

The initial description of sea surface elevation, currents, salinity and temperature is taken from the DNMI-IMR diagnostic climatology (Engedahl *et al.*, 1995). At the open boundaries this is complemented by the four tidal constituents  $K_1$ ,  $M_2$ ,  $N_2$  and  $S_2$ . The tidal data are compiled at DNMI on the basis of model results from Flather (1981), Gjevik & Straume (1989), and Gjevik *et al.* (1990). The meteorological forcing is taken from the hindcast archive of DNMI (Eide *et al.*, 1985). This consist of analysed air pressure on a 75 km grid covering the Nordic Seas.

In lack of data on heat exchange between the ocean and atmosphere, a simple approach of Cox & Bryan (1984) is used. Based on the difference between the sea surface temperature computed by the model and in the climatology, a heat flux is prescribed forcing the model towards the climatology on a time scale of a couple of weeks. This procedure gives a reasonable seasonal temperature cycle. On the other hand, it makes the surface temperature not purely prognostic.

The precipitation minus evaporation is set to zero. Rivers are included as sources for freshwater and volume. 27 Norwegian and 20 rivers from other countries are included. The river outflow data are compiled on a monthly basis with realistic seasonal cycle. For some rivers actual data for each simulation year are available, for others a climatology or a specific year has been used for all simulations.

The inflow from the Baltic is implemented after an algorithm due to Stigebrandt (1980). This flow is determined from the difference in modelled water level between the southern Kattegat and the Baltic, taking into account climatological freshwater input to the Baltic.

## **3. THE LARVAE TRANSPORT MODEL**

### **3.1 Generalities**

In the transport model particles are released and transported in space and time to simulate the drift of capelin larvae. The transport processes are modelled by a simple Lagrangian particle tracking model. The model is driven by the stored daily mean (25 hour) current velocity fields from the circulation model. These fields are interpolated in time and used to move the particles to their next position in an “Euler forward” way. Spatial variability in the current field leads to a spreading of the particles. The spreading on smaller scale is parameterised by random walk diffusion, where each particle is given a velocity every time step based on an axi-symmetric Gaussian random factor and the standard deviation of the horizontal velocity components. For more details on the transport model see Ådlandsvik & Sundby (1994); Hansen & Ådlandsvik (1996).

No mortality has been introduced in the model. If a particle is carried by the current into a land grid cell it is moved to the closest sea cell.

### **3.2 Model setup**

The transport model has been run from 23 April to 1 October in the years 1988-91. The transport model domain is shown in figure 3.1. The horizontal resolution is 20 km and the number of grid cells is  $95 \times 95$ .

The particles are released in 11 known spawning areas (Harald Gjøsæter pers. comm.) situated along the coast of Troms and Finnmark as shown in figure 3.1. The model hatching curves are similar in all sites. The hatching is divided into three five day periods. The first starts 24 April with 25 particles released each day. In the next period 50 particles are released each day and in the last 25. This adds up to a total number of 500 particles in each site. The use of the same hatching curves each year means that the model results show the year-to-year variabilities caused directly by the modelled currents, and do not account for possible biological year-to-year variations in factors such as mortality, number of hatched larvae, etc.

The modelling of the vertical behaviour of the larvae is uncertain since few observations have

been made. However, in Fossum & Bakkeplass (1991) and also in Fossum & Bakkeplass (1989) the vertical distribution during one day has been studied. Based on the observations in Fossum & Bakkeplass (1991) a 24 hour cycle has been deduced. The depths in metets are as follows, starting from midnight: 35, 35, 35, 37, 40, 42, 45, 45, 45, 37, 35, 32, 30, 30, 30, 25, 22, 20, 18, 18, 20, 22, 25, 30. Comparisons with simulations with other vertical migration schemes are shown in section 5.3.

The random walk diffusion is implemented by adding random velocity components to the deterministic velocity components from the current fields. These random components are drawn from central normal distributions with standard deviation  $ustdev$  and  $vstdev$  in  $x$ - and  $y$ -direction respectively. This corresponds to a Fickian diffusion coefficient  $K$  given by

$$2K = ustdev^2 \Delta t, \quad (3.1)$$

see (Hansen & Ådlandsvik, 1996).

In this work two descriptions of  $ustdev$  has been used. First, as in Ådlandsvik & Sundby (1994),  $ustdev$  is computed from a constant value of  $K$  by equation (3.1). The second approach, used in Svendsen *et al.* (1995), computes  $ustdev$  from the variance  $uvar$  and  $vvar$  of the velocity components during a  $M_2$  tidal cycle. More precisely,  $ustdev = \sqrt{facdiff * uvar}$ . Here  $facdiff$  is a dimensionless parameter. This formulation gives a non-uniform diffusion rate in space and time with more diffusion with high current variability. Since the components are treated separately, the diffusion is non-isotropic.

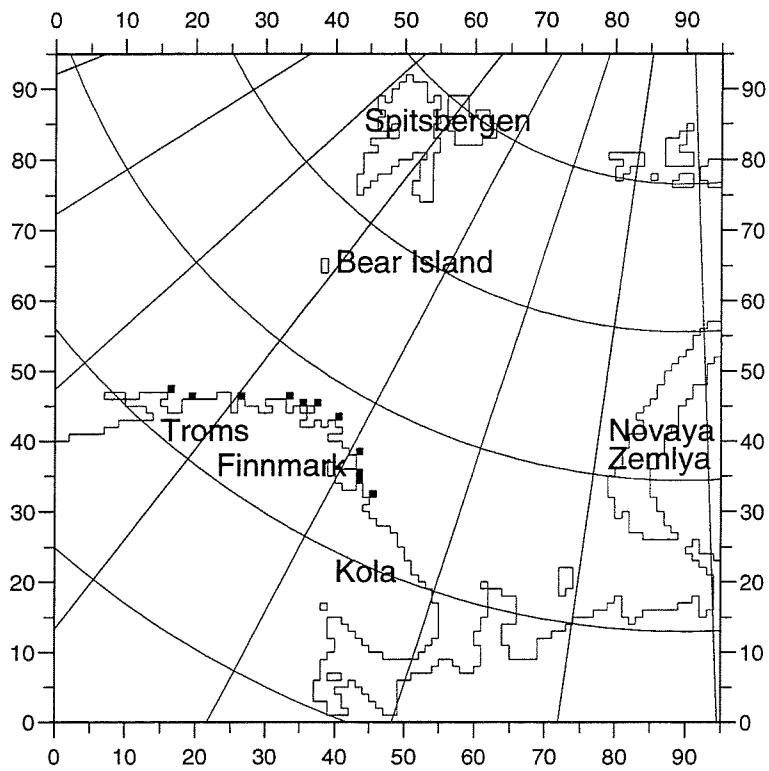


Figure 3.1: Transport model domain with spawning sites. From west to east: Andenes, Malangsgrunnen, Loppa, Tarhalsen, Ingøya, Magerøya, Nordkynnhalvøya, Blodskyttodden, Kiberg, Varangerfjorden, and Fiskerhalvøya.

## 4. RESULTS FROM THE CIRCULATION MODEL

### 4.1 Current conditions

Figure 4.1 from Loeng *et al.* (1997) shows the mean surface circulation based on observations. By comparing this with the modelled monthly mean currents in 10 m in 1989 given in figure 4.2 it is clear that several of the main features in the circulation are reproduced in the model.

In the western part of the area the Norwegian Atlantic Current along the shelf edge splits into one part going northwards as the West Spitsbergen Current and one part entering the Barents Sea as the North Cape Current. The North Cape Current again splits into two branches in figure 4.1, with one going northeastwards east of the Bear Island and one going eastwards as the Murman Current. The former has not been reproduced in the model. But the Murman Current is present in all months and with an especially clear continuation along the west coast of Novaya Zemlya in May. The Coastal Current along the coast of Northern Norway flows mainly eastwards in both the observed and modelled circulation but the eddies are not seen as clearly in the model.

The main difference between the modelled results and the standard view is however in connection with the Arctic Water flowing into the area from the north and east between Spitsbergen, Franz Joseph's Land and Novaya Zemlya. Compared to the currents flowing southeastwards in the northern Barents Sea in figure 4.1 the modelled currents are too weak.

As shown in figure 2.1 the currents are computed on a larger domain than the Barents Sea. This is done for the EU-project TASC, (TransAtlantic Study of Calanus). For a presentation of the modelled current fields outside the Barents Sea, see Ådlandsvik & Eriksrød (1997).

### 4.2 Horizontal diffusion coefficient

Figure 4.3 gives an example of the horizontal diffusion coefficients  $K_{xx}$  and  $K_{yy}$  calculated with equation (3.1) based on modelled  $ustdev$  and  $vstdev$  in the uppermost layer on a randomly chosen day (2 February 1989). The diffusion coefficient is highest in the area around Bear Island and Hopen Island and in the outlet of the White Sea and further east along the Russian coast. This is also the areas with strongest tidal currents (Gjevik *et al.*, 1994). In the central Barents Sea, typical values are in the order of 20–80  $m^2s^{-1}$ .

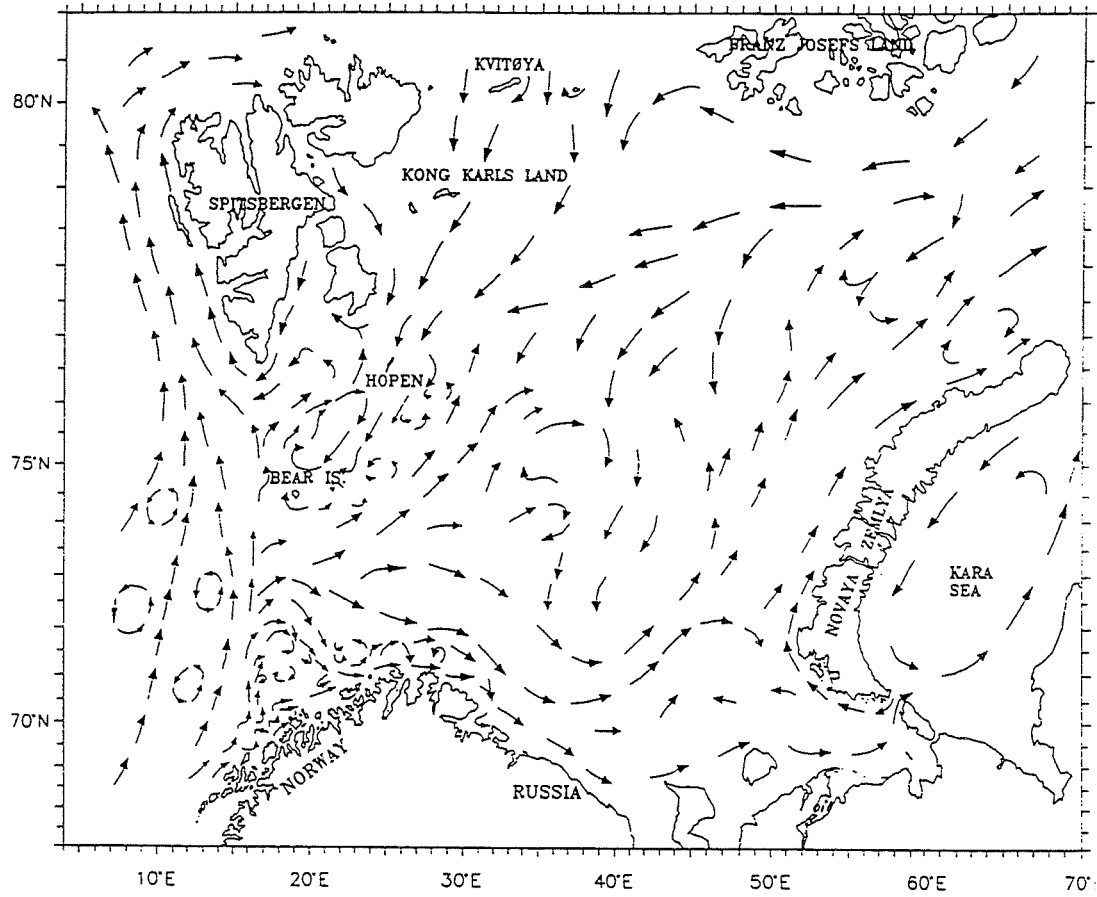


Figure 4.1: Mean surface circulation map from the Barents Sea, after Loeng *et al.* (1997)

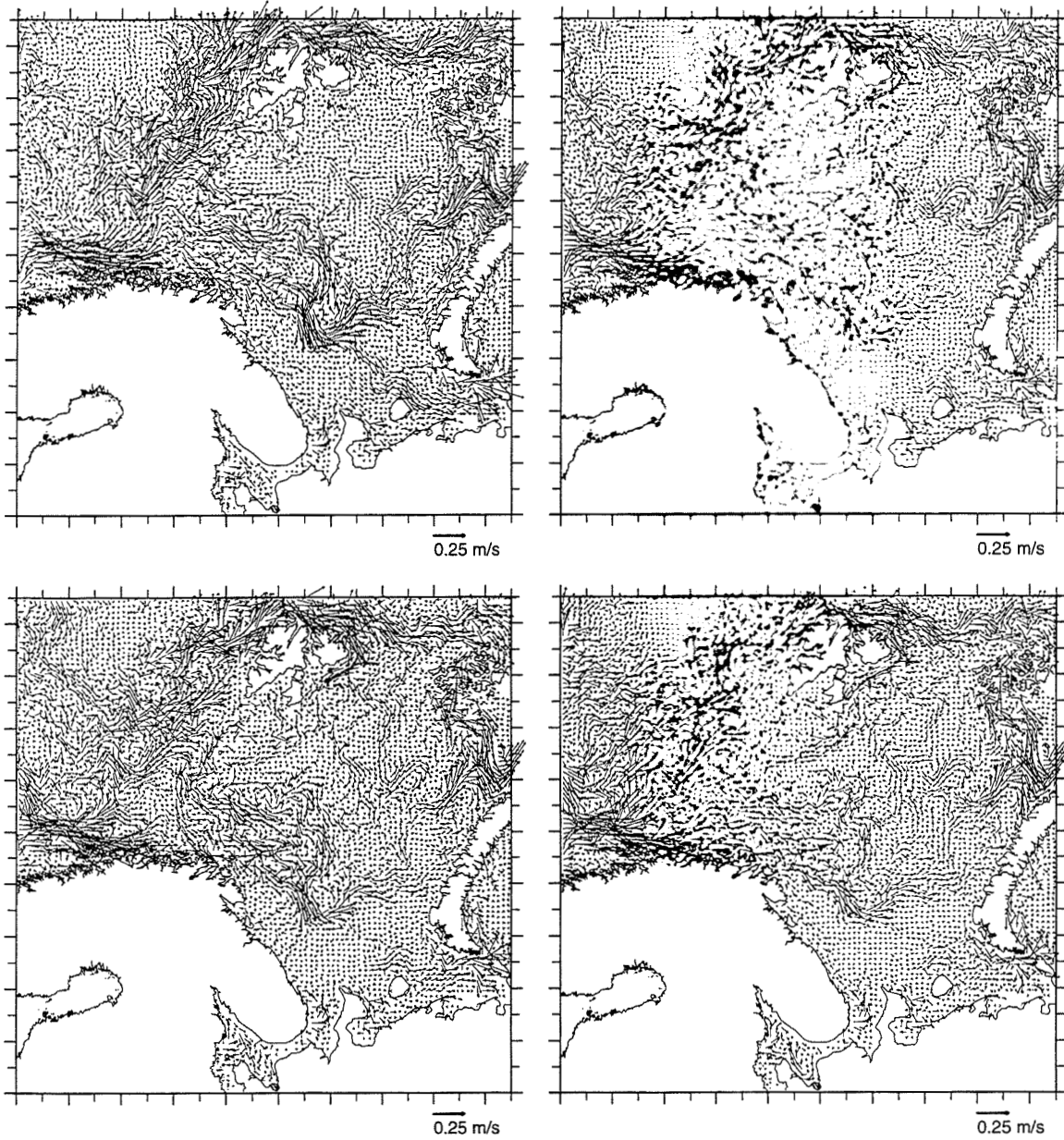
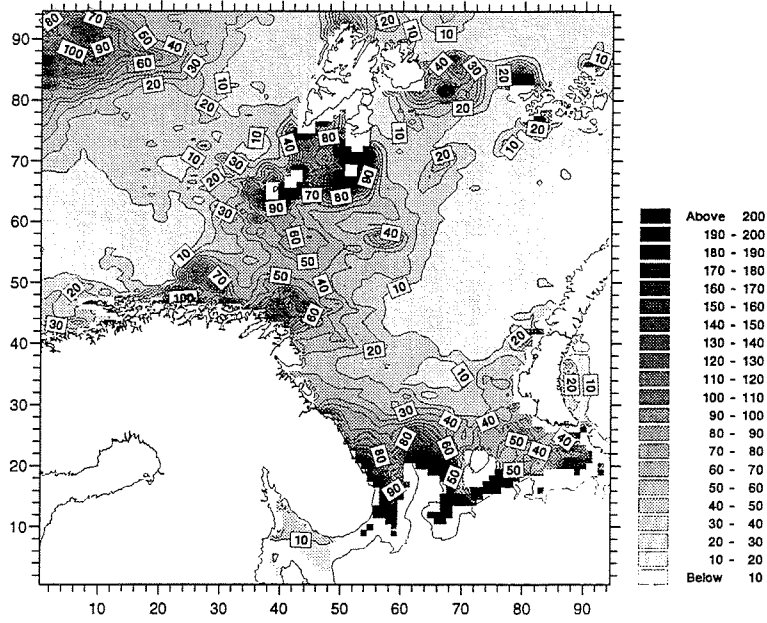
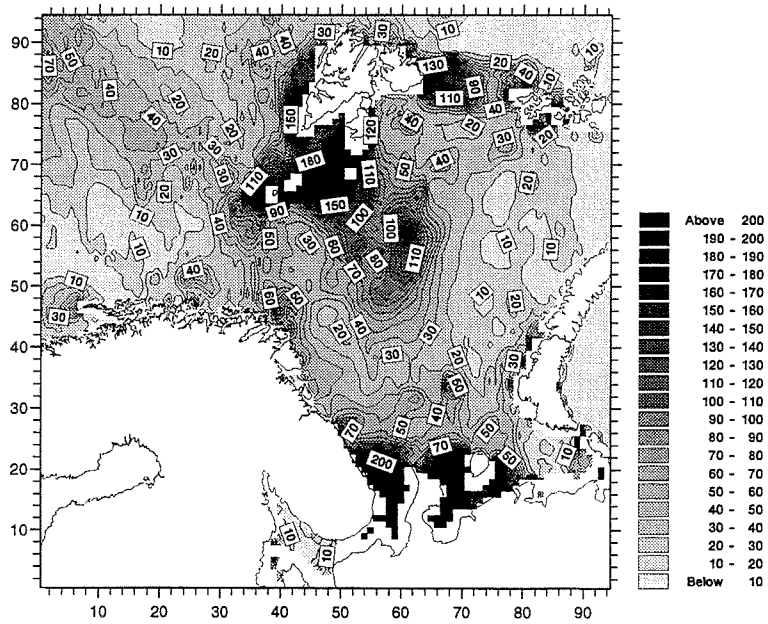


Figure 4.2: The monthly mean modelled current at 10 m in May, June, July and August 1989.



(a)  $K_{xx}$



(b)  $K_{yy}$

Figure 4.3: The horizontal diffusion coefficients (units in  $\text{m}^2\text{s}^{-1}$ ).

## **5. RESULTS FROM THE TRANSPORT MODEL**

### **5.1 Comparison with observations**

The simulations are performed with parameters described in the model setup in section 3. Since no mortality is present in the model, and since no knowledge of the number of actual hatched larvae is available for individual years, it is not possible to do a direct comparison between the model concentrations and the observations. Basically we compare the distribution and drift patterns of observed larvae vs. modeled particles, and not the actual numbers of larvae.

In the four years the transport model has been run observations of the distribution of capelin larvae has been made in June and in the 0-group surveys in August/September. In addition observations have been made on cruises in March/April, close to the spawning time.

#### **Distribution in 1988**

In Fossum (1988) the larvae distribution in June shows large concentrations at Tarhalsen, west and east of Nordkynnhalvøya and in and outside Varangerfjorden. These observations indicate that hatching has taken place along most of the coast. However, no stations are taken further south than Tarhalsen.

The observed 0-group distribution in figure 5.1 from Anon (1988) shows that 0-group capelin are spread over large parts of the Barents Sea almost as far north as 77°N with main concentrations in the area from 71°N to 72°30'N and 30°E to 34°E. The western-most larger area of observations are found on the shelf with few observations along the shelf edge northwards to Spitsbergen.

Comparison with the modelled distribution in figure 5.2 shows that the model fails to simulate the transport of larvae north/northeast from the coast out into the Barents Sea. The model shows large concentration of larvae mainly hatched at Andenes along the slope to Spitsbergen and to the east on the shelf. Otherwise the model shows that larvae from Nordkynnhalvøya, Tarhalsen, Ingøya and Magerøya are transported with the Murman current in the area where the largest concentrations of larvae are observed.

## **Distribution in 1989**

In Fossum & Bakkeplass (1989) the larvae distribution in June shows larger concentrations than in 1988 all along the coast with especially large amounts from Nordkynnhalvøya to the Varanger fjord. Also in this year no stations are taken further south than Tarhalsen.

In figure 5.3 from Anon (1989) large concentrations of 0-group capelin can be seen covering large parts of the Barents Sea from the coast up to 77°N and from 17° to 46°E. In addition there are also scattered observations of high concentrations along the shelf edge up to Spitsbergen.

In the modelled simulation there are very few larvae along the shelf edge. The larvae from the southern spawning grounds are in contradiction to the case in 1988 transported into the Barents Sea. The model still fails to simulate the transport of larvae hatched on the coast of Finnmark into the Barents Sea.

## **Distribution in 1990**

The larvae distribution in June shows large amounts of larvae east of Nordkynnhalvøya and very reduced concentrations west of Magerøya (Fossum & Bakkeplass, 1991). In a cruise report (Anon, 1990b) in March very small amounts of larvae were observed west of Ingøy.

In figure 5.5 from Anon (1990a) the largest concentration of 0-group capelin has moved far out from the coast and is found between 73° and 76°30'N.

In the modelled distribution large amounts of larvae are found along the slope but since spawning probably has taken place at the eastern part of the coast, larvae cannot be expected to be found here in the observations. As in the previous years the larvae are hardly transported northwards from the coast.

## **Distribution 1991**

The larvae distribution in June is mainly focused between Tarhalsen and Ingøya and from Nordkynnhalvøya to the Varanger fjord (Harald Gjørseter pers. comm.)

In figure 5.7 from Anon (1991) the distribution of 0-group capelin is very scattered and the observations are made far north with hardly no observations near the coast. High concentration is also seen outside the west coast of Spitsbergen.

In the modelled distribution larvae from Andenes has been transported north of 76°N to the west coast of Spitsbergen. The eastern boundary is further east this year than the previous ones. As before the drift towards north-northeast has not been resolved by the model.

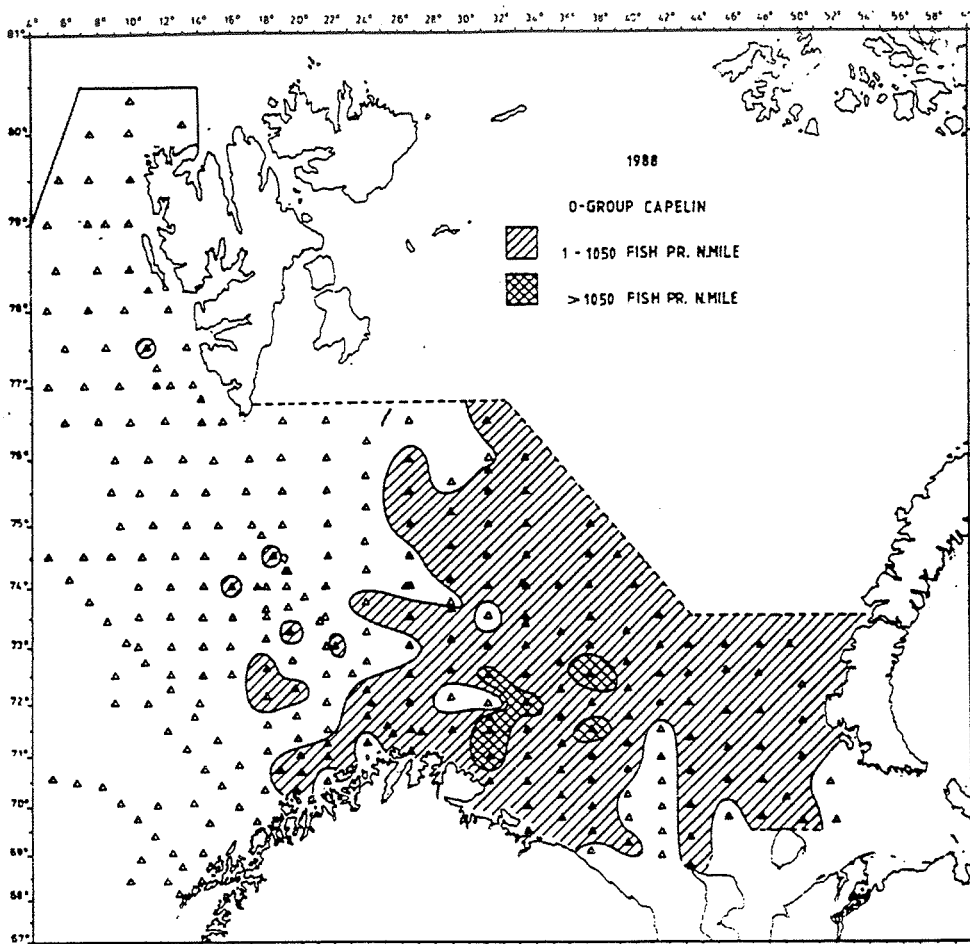


Figure 5.1: The observed 0-group distribution in August/September 1988.

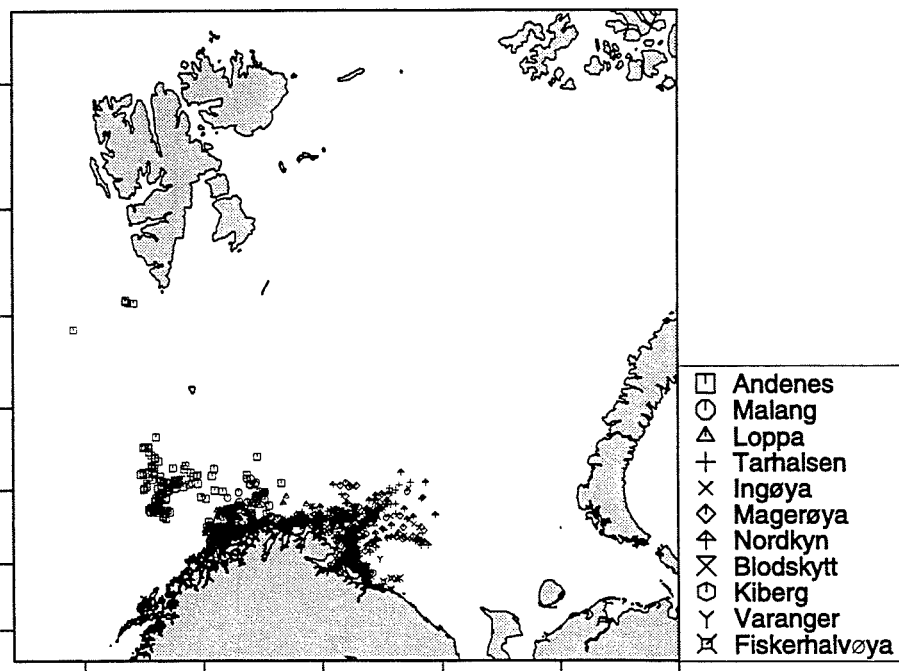


Figure 5.2: The modelled larvae distribution on 1 September 1988. The different symbols distinguishes between the spawning areas according to the legend.

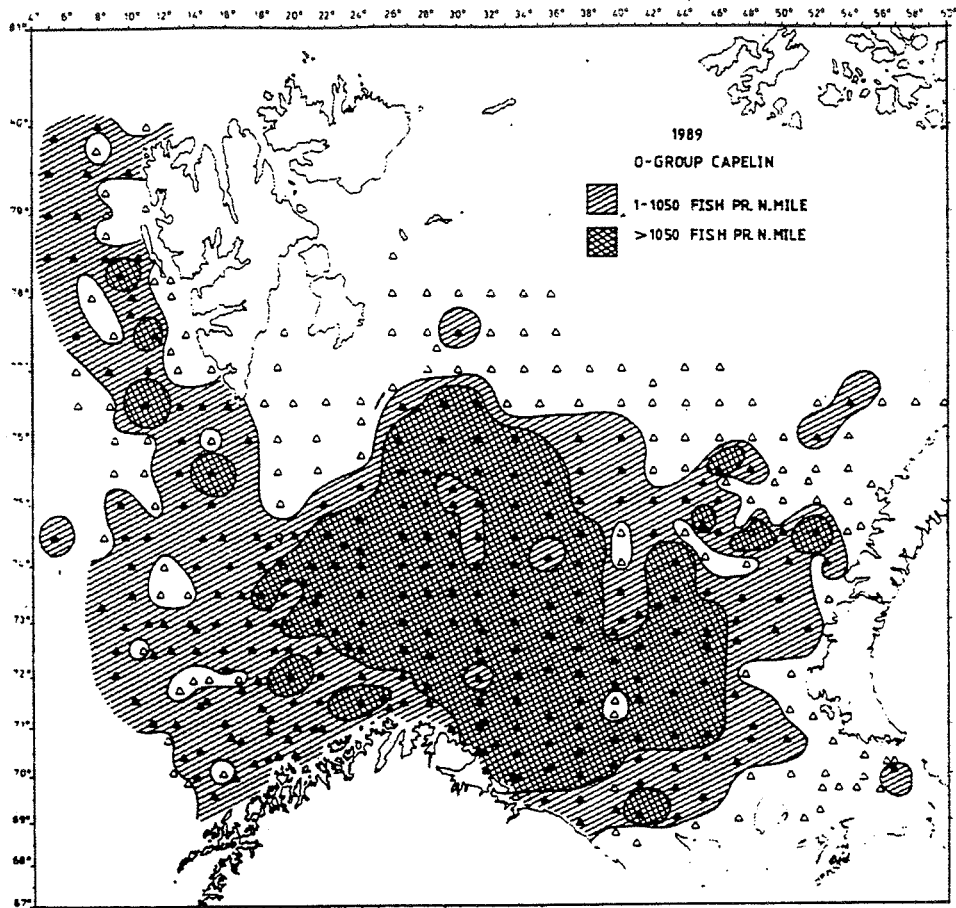


Figure 5.3: The observed 0-group distribution in August/September 1989.

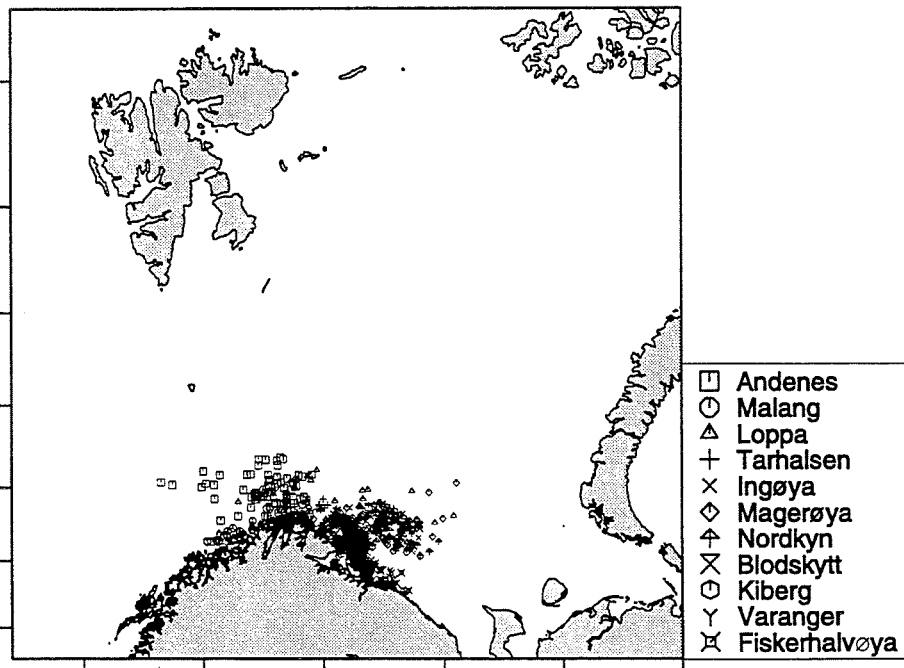


Figure 5.4: The modelled larvae distribution on 1 September 1989.

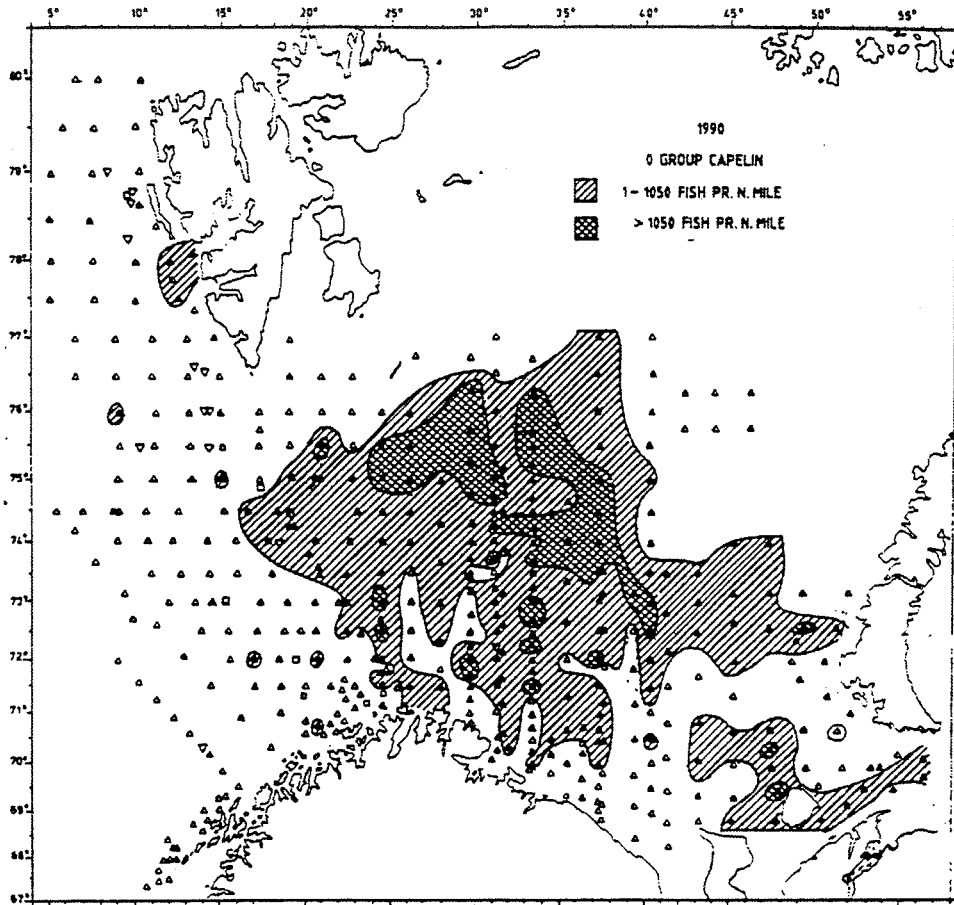


Figure 5.5: The observed 0-group distribution in August/September 1990.

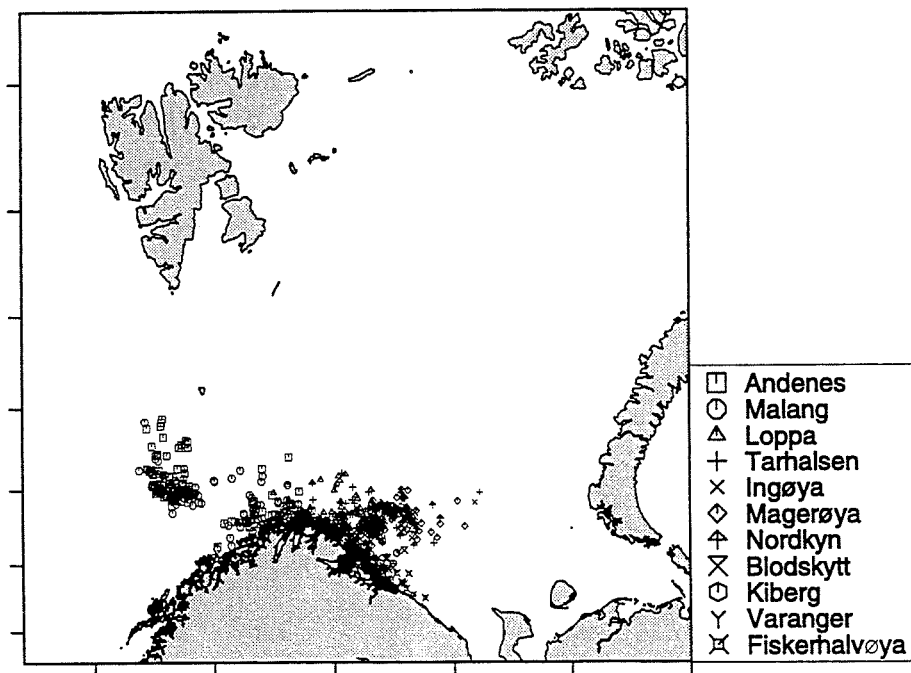


Figure 5.6: The modelled larvae distribution on 1 September 1990.

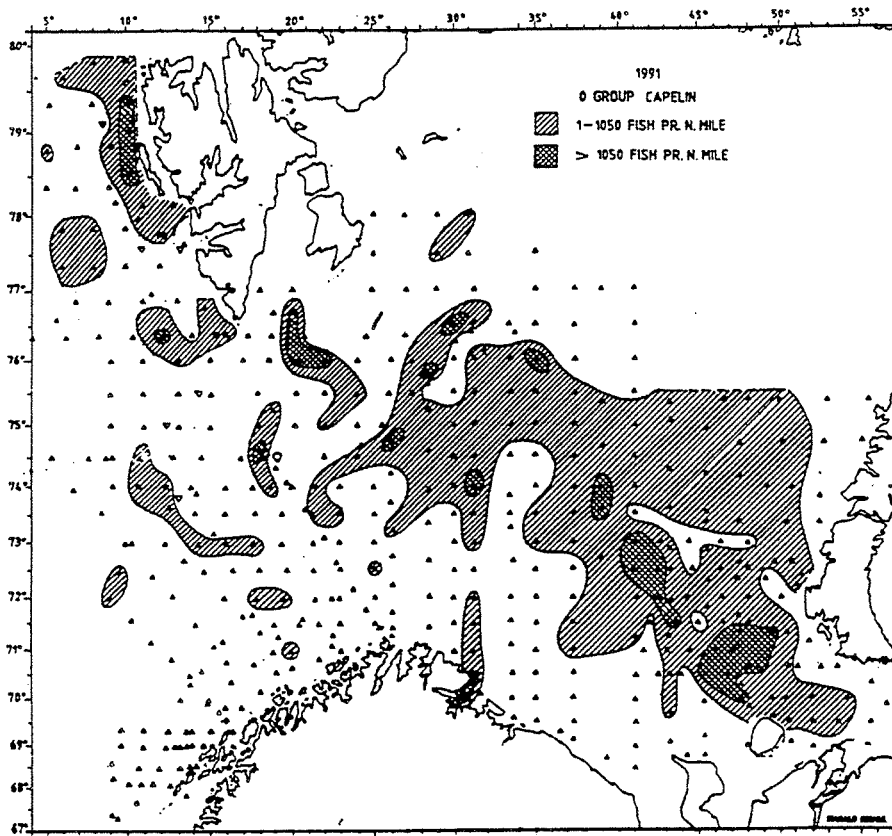


Figure 5.7: The observed 0-group distribution in August/September 1991.

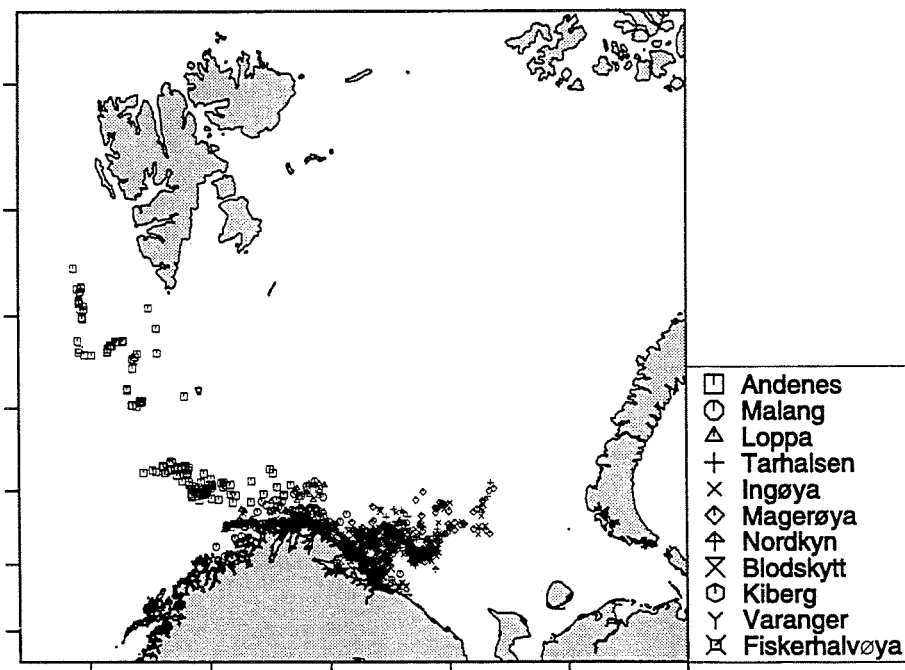


Figure 5.8: The modelled larvae distribution on 1 September 1991.

## 5.2 Comparison of different horizontal diffusion parametrizations

In this section, the same current fields are kept but the parametrization of horizontal diffusion is varied. From earlier experience (Ådlandsvik & Sundby, 1994) it is expected that the spreading of the particles is sensitive to this parametrization.

In section 3.2 two ways for parametrization of the standard deviation of the horizontal random walk velocity components were described. Here four simulations have been run, two with the variance formulation (figure 5.4 and figure 5.9) and two with fixed standard deviation (figure 5.10 and figure 5.11). The parameter settings are summarised in table 5.1.

Figure	Formulation	facdiff	K	Variance
5.4	Variance	1	-	99.9
5.9	Variance	4	-	119.4
5.10	Constant	-	50	115.4
5.11	Constant	-	500	216.6

Table 5.1: Overview of the diffusion sensitivity runs and the variance of the resulting particle distribution on 1 September. The unit for K is  $\text{m}^2\text{s}^{-1}$  and the unit for variance is grid cell area ( $4 \times 10^8 \text{ m}^2$ ).

The results presented in Figures 5.9 and 5.10 do not differ much from the standard run given in figure 5.4. As seen in table 5.1 the variances of the distributions are also quite similar.

In the case of  $K = 500 \text{ m}^2\text{s}^{-1}$  (figure 5.11), the larvae are more dispersed. The northern boundary has passed  $74^\circ\text{N}$  and more larvae have been transported along the slope from northern Norway to Spitsbergen.

These results indicate that increasing the horizontal diffusivity within reasonable bounds do not help very much to transport the larvae as far north as  $76^\circ\text{N}$ . Further increase of the diffusion will spread the particles randomly in the Barents Sea and will not give more information on the transport process.

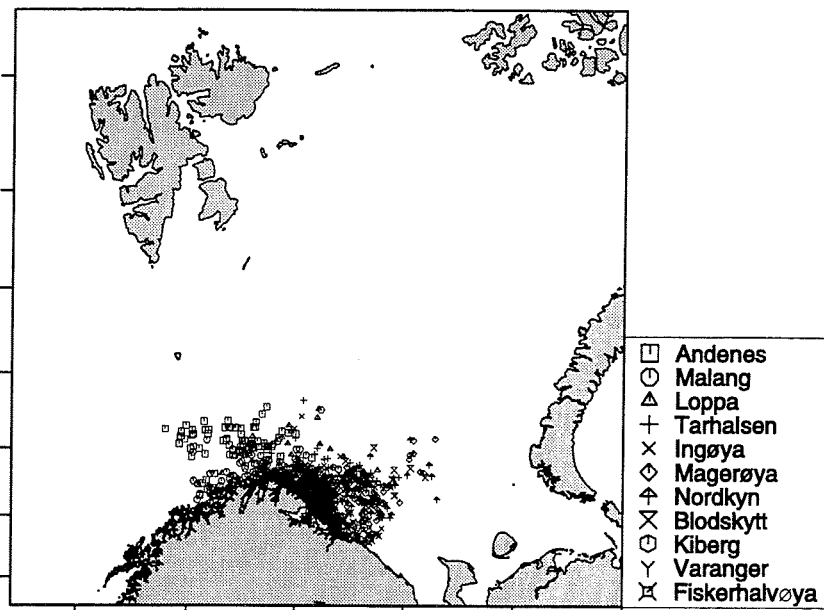


Figure 5.9: The modelled larvae distribution on 1 September with variance formulation and  $\text{facdiff} = 4$ .

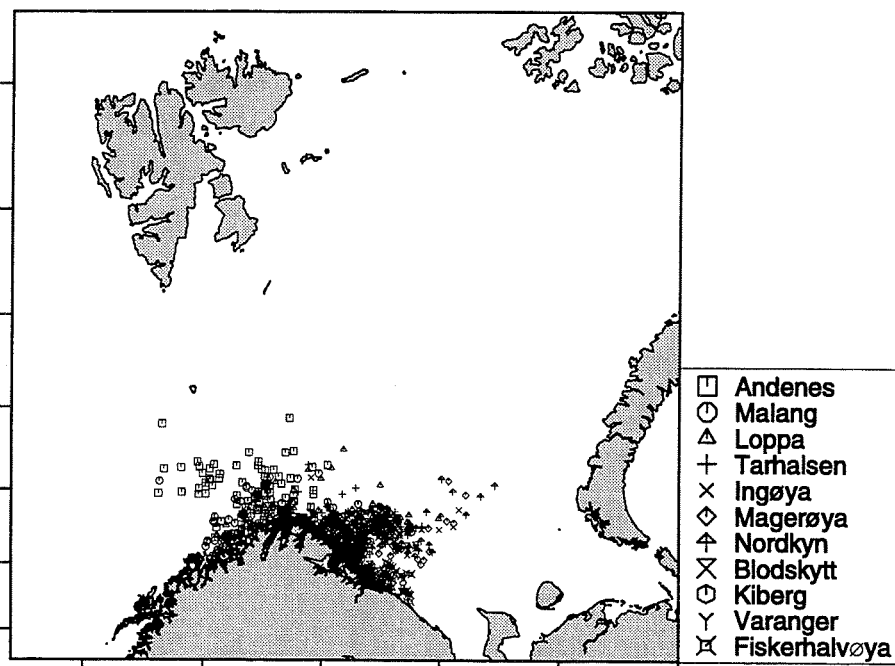


Figure 5.10: The modelled larvae distribution on 1 September with constant  $K = 50$ .

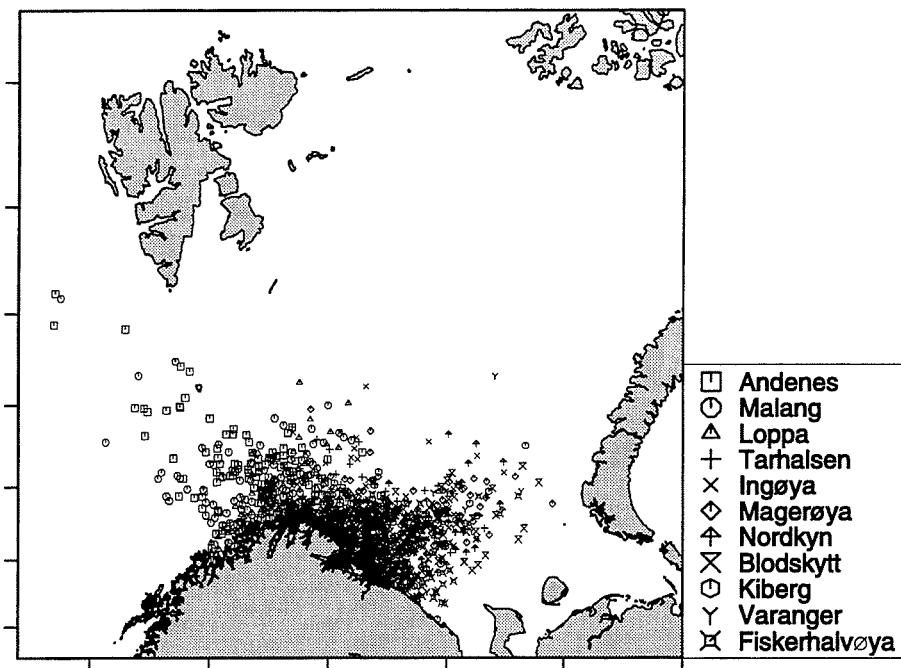


Figure 5.11: The modelled larvae distribution on 1 September with constant  $K = 500$ .

### 5.3 Comparison of different vertical migration schemes

In addition to comparing results from simulations with different horizontal diffusion, the sensitivity to different vertical migration schemes are studied. Two simulations with the larvae kept fixed in 10 m and 30 m are compared to the results in figure 5.10 with a 24 hour cycle vertical migration. In all three simulations a fixed horizontal diffusion coefficient of  $K = 50 \text{ m}^2\text{s}^{-1}$  is used. The model experiments are summarized in table 5.2.

Figure	Vertical movement	Variance
5.10	Vertical migration	115.4
5.12	Fixed at 10 m	155.4
5.13	Fixed at 30 m	122.7

Table 5.2: Overview of the vertical migrations sensitivity runs and the variance of the resulting particle distribution on 1 September. The unit for the variance is grid cell area ( $4 \times 10^8 \text{ m}^2$ ).

The wind forcing on the ocean produces more variable current conditions near the surface. It is therefore expected that the 10 m simulation (5.12) should give the largest horizontal extent of the distribution. This is confirmed by table 5.2 with higher variance in this case. The difference, however, is not large and is not apparent from the figures. With the present current fields, the results are not very sensitive to the vertical migration pattern used.

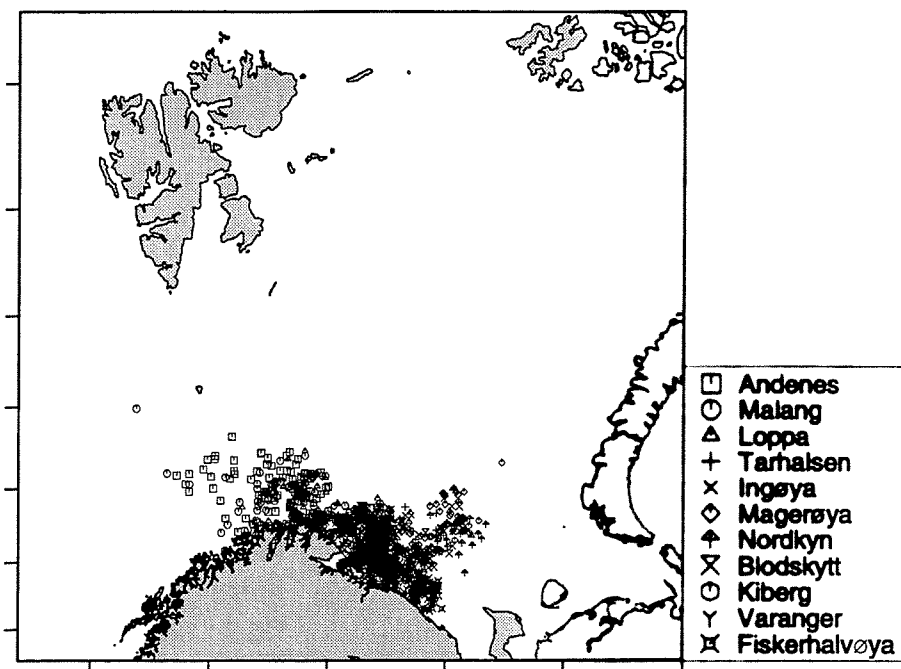


Figure 5.12: The modelled larvae distribution on 1 September with larvae kept fixed at 10 m.

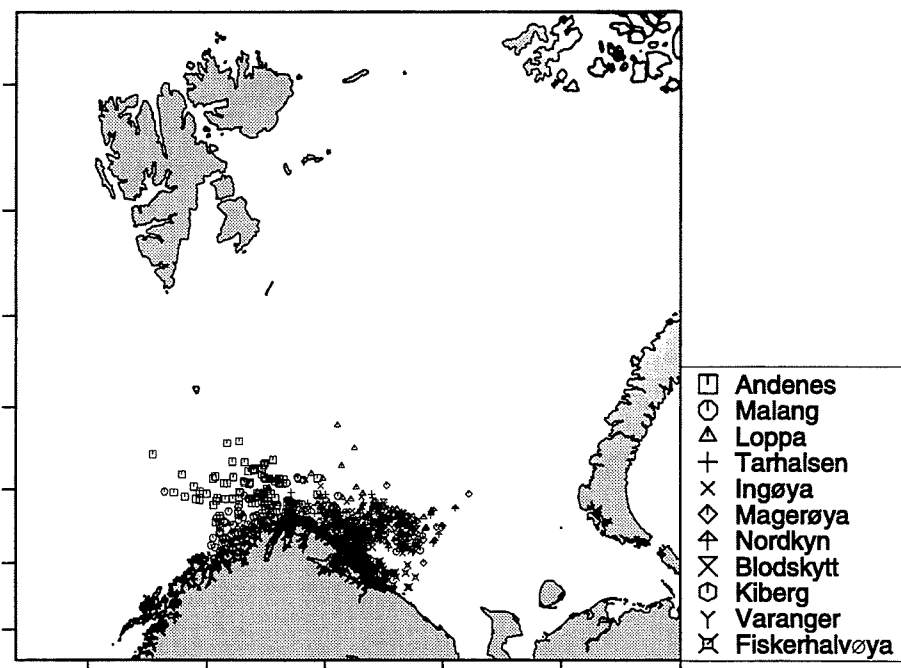


Figure 5.13: The modelled larvae distribution on 1 September with larvae kept fixed at 30 m.

## 6. DISCUSSION AND CONCLUSION

The comparisons between modelled and observed 0-group distributions in section 5.1 shows that the model produces too high larval concentrations near the coast. More seriously, the model totally fails to reproduce the northwards extent of the observed distributions. Possible explanations of this discrepancy are discussed below.

Mortality is not included in the transport model. If the mortality is space dependent, model particles may be transported to areas where most of the real larvae has died. If the mortality is higher near the coast, this may explain why the observed 0-group distributions in 1990 and in particular 1991 have such low concentrations near the coast. However, lack of mortality can not explain why no particles are found far enough to the north in the model.

Another neglected biological mechanism is horizontal swimming. In the simulations of Werner *et al.* (1993) swimming helped to retain the modelled cod larvae on Georges Bank. However, swimming from 74°N to 76°N, more than 200 km in less than half a year requires a systematic northwards swimming speed of more than 1  $\text{cm s}^{-1}$ . This does not sound very realistic for capelin larvae.

Another explanation may be bad parametrisation of the transport model. This is examined by the sensitivity studies in sections 5.2 and 5.3. Here it is shown that changing the horizontal diffusion coefficient (within reasonable bounds) or the vertical migration pattern does not help much to reproduce the northwards extent of the real larvae distributions.

The most probable explanation lies in the current fields that is driving the larval model. However, the comparison in section 4.1 showed reasonably good agreement between mean observed and modelled monthly mean horizontal currents in the southern and central parts of the Barents Sea. Also from the conventional surface current pattern (fig. 4.1) it is difficult to explain the drift of larvae northwards across the main current direction.

Therefore, it is reasonable to believe that the drift northwards is produced by velocity components normal to the coast on a short time scale, i. e. tidal currents, even though they are not very strong along this part of the coast (Kowalik & Proshutinsky, 1995). However, the mean current is weaker in this area than further south which means that the tidal currents may be of larger relative importance. The observed distributions of larvae in section 5.1 with large horizontal extension also suggest that the larvae are spread rather than advected with main currents. In the North Sea the vertical migration of herring larvae has been connected to tidal cycle (Heath *et al.*,

1991; Bartsch, 1993). If capelin larvae uses a similar behaviour, the systematic contribution of the tidal current can be increased.

Another important source of error is the relatively crude grid resolution of 20 km which means that smaller scale details in the circulation pattern is not reproduced in the model. With the same model in the Svalbardbanken area, increased resolution to 4 km greatly improved the quality of the modelled current fields (Ådlandsvik & Hansen, 1997). Due to low density of measurements it is likely that such small scale features are also missing in the conventional current picture.

## BIBLIOGRAPHY

- ÅDLANDSVIK, B., & ERIKSRØD, G. 1997. *A hindcast simulation of currents in the Nordic Seas*. Fisken og Havet, xx: 1997, Havforskningsinstituttet. (in preparation).
- ÅDLANDSVIK, B., & HANSEN, R. 1997. Numerical simulation of the circulation in the Svalbardbanken area in the Barents Sea. *Cont. Shelf. Res.* (accepted).
- ÅDLANDSVIK, B., & SUNDBY, S. 1994. Modelling the Transport of Cod Larvae from the Lofoten Area. *ICES mar. Sci. Symp.*, **198**, 379–392.
- ANON. 1988. *Preliminary report of the international 0-group fish survey in the Barents Sea and adjacent waters in August-September 1988*. ICES C.M. 1988/G:45.
- ANON. 1989. *Preliminary report of the international 0-group fish survey in the Barents Sea and adjacent waters in August-September 1989*. ICES C.M. 1989/G:40.
- ANON. 1990a. *Preliminary report of the international 0-group fish survey in the Barents Sea and adjacent waters in August-September 1990*. ICES C.M. 1990/G:46.
- ANON. 1990b. *Toktrapport, tokt nr. 5 1990*. Tech. rept. Institute of Marine Research.
- ANON. 1991. *Preliminary report of the international 0-group fish survey in the Barents Sea and adjacent waters in August-September 1991*. ICES C.M. 1991/G:50.
- BARTSCH, J. 1993. Application of a circulation and transport model system to the dispersal of herring larvae in the North Sea. *Cont. Shelf Res.*, **13**, 1335–1361.
- BERNTSEN, J., SKAGEN, D. W., & SVENDSEN, E. 1994. Modeling the transport of particles in the North Sea with reference to Sandeel larvae. *Fish. Oceanogr.* **3**: 2, 81–89.
- BLUMBERG, A.F., & MELLOR, G.L. 1987. A description of a three-dimensional coastal ocean circulation model. In: HEAPS, N. (ed), *Three-Dimensional Coastal Ocean Models*. Coastal and Estuarine Sciences, vol. 4. American Geophysical Union.
- BOGSTAD, B., HIIS HAUGE, K., & ULLTANG, Ø. 1997. MULTSPEC – A multispecies model for fish and marine mammals in the Barents Sea. *J. Northw. Atl. Fish. Sci.* (accepted).

- COX, M.D., & BRYAN, K. 1984. A Numerical Model of the Ventilated Thermocline. *J. of Physical Oceanography*, **14**, 674–687.
- EIDE, L.I., REISTAD, M., & GUDDAL, J. 1985. *Database av beregnede vind og bølgeparametre for Nordsjøen, Norskehavet og Barentshavet, hver 6. time for årene 1955–81*. Tech. rept. The Norwegian Meteorological Institute.
- ENGEDAHL, H. 1995. Use of the flow relaxation scheme in a three-dimensional baroclinic ocean model with realistic topography. *Tellus*, **47A**, 365–382.
- ENGEDAHL, H., ÅDLANDSVIK, B., & MARTINSEN, E.A. 1995. *Production of monthly mean climatological archives of salinity, temperature, current and sea level for the Nordic Seas*. Research Report No. 3, The Norwegian Meteorological Institute.
- FIKSEN, Ø., GISKE, J., & SLAGSTAD, D. 1995. A spatially explicit fitness-based model of capelin migrations in the Barents Sea. *Fish. Oceanogr.*, **4**, 193–208.
- FLATHER, R.A. 1981. Results from a model of the north-east Atlantic relating to the Norwegian Coastal Current. *Pages 427–458 of: SÆTRE, R., & MORK, M. (eds), The Norwegian Coastal Current*, vol. 2. University of Bergen.
- FOSSUM, P. 1988. *Loddelarveundersøkelsene - 1988*. Tech. rept. 21. Institute of Marine Research.
- FOSSUM, P., & BAKKEPLASS, K. 1989. *Loddelarveundersøkelsene*. Tech. rept. 26. Institute of Marine Research.
- FOSSUM, P., & BAKKEPLASS, K. 1991. *Loddelarveundersøkelsene - 1990*. Tech. rept. 39. Institute of Marine Research.
- FOSSUM, P., & ØIESTAD, V. 1991. *De tidlige livsstadiene hos fisk i møte med trusselen fra petroleumsvirksomheten, sluttrapport fra Havforskningsinstituttets egg- og larveprogram - HELP 1985–1991*. Tech. rept. Institute of Marine Research.
- GISKE, J., SKJOLDAL, H.R., & AKSNES, D.L. 1992. A conceptual model of distribution of capelin in the Barents Sea. *Sarsia*, **77**, 147–156.
- GJEVIK, B., & STRAUME, T. 1989. Model simulation of the  $M_2$  and  $K_1$  tide in the Nordic Seas and Arctic Ocean. *Tellus*, **41**, 73–96.

- GJEVIK, B., NØST, E., & STRAUME, T. 1990. *Atlas of tides on the shelves of the Norwegian and the Barents Seas*. Statoil report F&U-ST 90012.
- GJEVIK, B., NØST, E., & STRAUME, T. 1994. Model simulations of the tides in the Barents Sea. *J. Geophys. Res.*, **99**, 3337–3350.
- GJØSÆTER, H. 1995. Pelagic Fish and the Ecological Impact of the Modern Fishing Industry in the Barents Sea. *Arctic*, **48**, 267–278.
- HANSEN, R., & ÅDLANDSVIK, B. 1996. *Application of a hydrodynamical model on transport of larvae of polar cod in the northern Barents Sea*. *Fisken og Havet*, 27: 1996, Havforskningsinstituttet.
- HEATH, M., BRANDER, K., MUNK, P., & RANKINE, P. 1991. Vertical distributions of autumn spawned larval herring (*Clupea harengus* L.) in the North Sea. *Cont. Shelf Res.*, **11**, 1425–1452.
- KOWALIK, Z., & PROSHUTINSKY, A. YU. 1995. Topographic enhancement of tidal motion in the western Barents Sea. *J. Geophys. Res.*, **100**, 2613–2637.
- LOENG, H., OZHIGIN, V., & ÅDLANDSVIK, B. 1997. *Water fluxes through the Barents Sea*. ICES J. mar. Sci. (in press).
- MARTINSEN, E.A., & ENGEDAHL, H. 1987. Implementation and Testing of a Lateral Boundary Scheme as an Open Boundary Condition in a Barotropic Ocean Model. *Coastal Engineering*, **11**, 603–627.
- MELLOR, G. L., & YAMADA, T. 1982. Development of a Turbulence Closure Model for Geophysical Fluid Problems. *Rev. Geophys. Space Phys.*, **20**, 851–875.
- MOKSNESS, E., SVENDSEN, E., & ERIKSØD, G. 1997. *Temporal and spatial occurrence of North Sea autumn spawned herring (*Clupea harengus*) larvae in the Skagerrak area: Comparison between field observations and drift model results*. (in preparation).
- SAKSHAUG, E., BJØRGE, A., GULLIKSEN, B., LOENG, H., & MEHLUM, F. (eds). 1994. *Økosystemet Barentshavet*. Universitetsforlaget, Oslo.
- SKOGEN, M.D. 1993. *A User's guide to NORWECOM, the NORwegian ECOlogical Model system*. Tech. rept. 6. Institute of Marine Research, Division of Marine Environment, Bergen.

- STIGEBRANDT, A. 1980. Barotropic and baroclinic response of a semi-enclosed basin to barotropic forcing of the sea. *Proceeding of the NATO Conference on Fjord Oceanography*, H. Freeland, D. Farmer, and C. Levings, eds., Plenum Press, New York.
- SVENDSEN, E., FOSSUM, P., SKOGEN, M.D., ERIKSRØD, G., BJØRKE, H., NEDREAAS, K., & JOHANNESSEN, A. 1995. *Variability of the drift patterns of Spring Spawmed herring larvae and the transport of water along the Norwegian shelf*. ICES C.M. 1995/Q:25.
- SVENDSEN, E., SKOGEN, M., MONSTAD, T., & COOMBS, S. 1996. *Modelling the Variability of the drift of blue whiting larvae and its possible importance for recruitment*. ICES C.M. 1996/S:31.
- TJELMELAND, S., & BOGSTAD, B. 1993. The Barents Sea Capelin Stock Collapse: A Lesson to Learn. *Can. Spec. Publ. Fish. Aquat. Sci.*, **120**, 127–139.
- WERNER, F.E., PAGE, F.H., LYNCH, D.R., LODER, J.W., LOUGH, R.G., PERRY, R.I., GREENBERG, D.A., & SINCLAIR, M.M. 1993. Influences of mean advection and simple behavior on the distribution of cod and haddock early life stages on Georges Bank. *Fish. Oceanogr.*, **2**, 43–64.